# Engineering structured light with optical vortices

**Jesús Rogel-Salazar,[1,2] Juan Pablo Treviño,[3] and Sabino Chávez-Cerda[3,*]**

[1]*Science and Technology Research Institute, School of Physics Astronomy and Mathematics, University of Hertfordshire, Hatfield, Hertfordshire, AL10 9AB, UK*

[2]*Blackett Laboratory, Department of Physics, Imperial College London, Prince Consort Road, London, SW7 2BZ, UK*

[3]*Instituto Nacional de Astrofísica, Óptica y Electrónica, Apartado Postal 51/216, Puebla, Pue., 72000, Mexico*

**Corresponding author: sabino@inaoep.mx*

Received January 8, 2014; revised March 25, 2014; accepted April 12, 2014;
posted April 25, 2014 (Doc. ID 204236); published May 20, 2014

In this work, we demonstrate the possibility of generating and controlling any given kind of structured radially symmetric intensity profile with an embedded optical vortex. This is achieved with the use of Sturm–Liouville theory on a circular domain with Bessel, Laguerre–Gauss, Zernike, and Fourier bases. We show that the core intensity profile can be constructed independently of the topological charge of the vortex. 

*OCIS codes:* (000.3860) Mathematical methods in physics; (000.4430) Numerical approximation and analysis; (350.5500) Propagation; (050.4865) Optical vortices; (350.4855) Optical tweezers or optical manipulation.
http://dx.doi.org/10.1364/JOSAB.31.000A46

## 1. INTRODUCTION

Electromagnetic vortices have become an active theme of research in the last two decades due to their association with the orbital angular momentum (OAM) of light and their wide spectrum of applications ranging from atom traps to optical tweezers, microscopy, optical communications, or astronomy [1–3]. Similarly, there has been increased interest in the use of structured light fields in various applications where control over the intensity profile is an advantage, such as in optical trapping [4] and three-dimensional measurements and printing [5], for example.

Vortex fields, known for carrying OAM, may arise naturally in the solutions of several differential equations (DEs) of mathematical physics, having an azimuthal dependence of the form $\exp(im\varphi)$ with $m$ being an integer that defines the topological charge of the vortex. For the paraxial wave equation the Laguerre–Gaussian (LG) functions are solutions of the paraxial wave equation and are well known for carrying OAM that is associated with its vortex solution [6]. This is just a particular case but any electromagnetic beam solution with a vortex component can carry OAM, as has been proved for Bessel beams which are described by the solutions of the Helmholtz equation in circular cylindric coordinates [7]. By looking at the 11 coordinate systems in which the Helmholtz equation is separable, we find that besides the Bessel solutions there are four other systems that yield separable vortex solutions: parabolic coordinates, prolate and oblate spheroidal coordinates, and the well-known spherical coordinates [8,9].

Wave equations of mathematical physics often lead to Sturm–Liouville (S-L) type DEs whose solutions are orthogonal functions [10–13]. These were recognized to have relevant properties used in communications more than half a century ago [14]. Optical vortices described by radial functions from a S-L DE can create two infinite-dimensional Hilbert spaces. One for the azimuthal index and the other for the orthogonal coordinate that for two-dimensional vortices is the radial index. By exploiting the OAM property of vortex fields, associated with the azimuthal index, these fields have been proposed as means of transmission of quantum information through entangled states expanding the possibilities of quantum cryptography and quantum communications [15,16]. Moreover, it has been suggested that the capacity of communications channels, cryptographic properties, and quantum algorithms can be improved by incorporating the radial modes Hilbert space of optical vortices [17].

In this work we show that it is possible to engineer structured vortex fields with tailor made radial intensity profiles by applying the S-L theory. Among the many possible bases, we have chosen four of them that are related to diffractive optics. Three of the bases studied here arise from DEs of the S-L type in a circular two-dimensional domain and they are the Bessel function (BF), the LG functions, and the Zernike polynomials (ZPs). The fourth one, comes from the well-known one-dimensional Fourier analysis but applied to the radial coordinate. We show that the resulting representation can be used for further investigating the imaging or propagation of these vortices.

## 2. BASIC STRUCTURE OF FUNDAMENTAL VORTICES

We will refer to fundamental vortex fields as those that are analytic solutions of a DE. Fundamental vortex fields have a radially symmetric ringed structure either finite or infinite, with their inner most ring radius depending on the parameters of the corresponding DE and its initial condition. Figure 1 shows the squared amplitude of radial profiles for vortices with the same topological charge $m = 5$. The first two rows show a set of LG modes of only one ring, $n = 0$ [Fig. 1(a)], and three rings, $n = 2$ [Fig. 1(b)], with reducing beams waist $w_0$ causing the reduction of the central ring radius in each case. Observe also that having more rings results in the reduction of

 

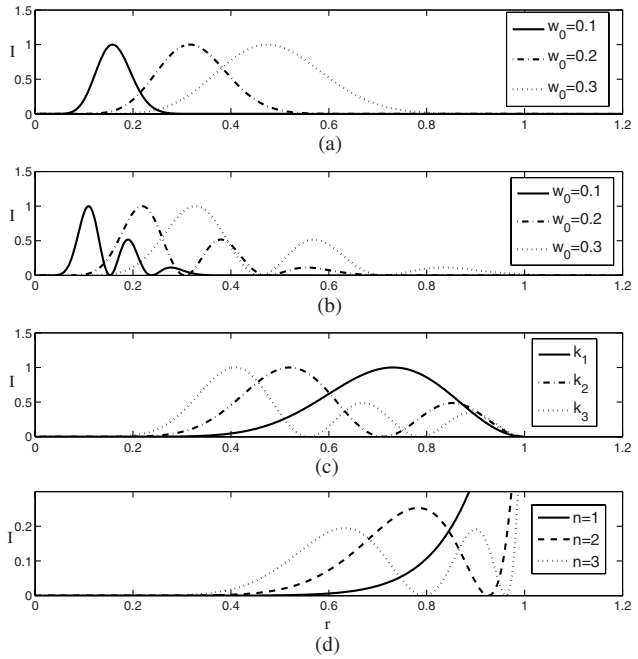


Fig. 1. (a) Laguerre–Gauss functions with azimuthal order $m = 5$ and radial order $n = 0$ showing the radial dependence of the profile on the Gaussian width; $w_0 = 0.1$, 0.2 and 0.3. (b) Laguerre–Gauss functions with same widths and $m = 5$ but radial order $n = 2$. (c) BFs of the same order $m = 5$ but increasing radial frequency $k_r$ corresponding to the first three eigenvalues. (d) ZPs with $m = 5$ and increasing radial order $n = 1$, 2, and 3.

the radii of the rings for the same $w_0$ used for a single ring. Figure 1(c) shows the ring radius dependence on the increasing radial frequency $k_r$ for BFs. Finally, Fig. 1(d) depicts the ZP showing the reduction of the ringed pattern with increasing radial order $n$. Thus, we conclude that for a physical vortex, it is the interplay between the radial and azimuthal parameters that control the radius of the vortex and not only the azimuthal one. We remark that this demonstrated behavior for a fixed topological charge contrasts with the recently introduced concept of the "perfect" optical vortex "whose dark hollow radius does not depend on the topological charge" [18]. We notice that for all of the cases shown in Fig. 1, even though the radius can be controlled, either in a continuous (LG) or a discrete way (BF and ZP), not so the shape of the profile, which is determined by the mode. In studies of transfer of OAM to microparticles it has been shown that besides the topological charge the velocity induced also depends on the intensity of the beam that carries the vortex [7]. In order to enhance the efficiency of transfer of OAM engineering, a desired profile for a vortex of a given topological charge $m$ would have potential applications [19]. For this purpose we recourse to the S-L theory in order to provide a suitable way to engineer generalized "perfect" vortices.

## 3. STURM–LIOUVILLE VORTICES

### A. Sturm–Liouville Theory

This theory establishes in simple words that any function $f(x)$ piecewise continuous square integrable in the interval $a \le x \le b$ can be expressed as

$$f(x) = \sum_{n=0}^{\infty} \langle u_n | f \rangle u_n(x), \tag{1}$$

where $\{u_n(x)\}(n = 0, 1, 2, \ldots)$ is an infinite set of eigenfunctions of a self-adjoint operator. They are mutually orthonormal with respect to the weight function $s(x)$, i.e.,

$$\langle u_m | u_n \rangle = \int_a^b u_m^*(x) u_n(x) s(x) \mathrm{d}x = \delta_{mn}, \tag{2}$$

and satisfy certain boundary conditions (BCs) at the ends of the interval $a \le x \le b$ of a S-L DE. If $f(x)$ satisfies the same BC as the basis functions, then the infinite series (1) converges uniformly and absolutely to $f$ in the interval. If $f$ does not satisfy the BCs then the series converges in the mean [10–13].

Optical vortices are characterized by functions of the separable type $A(r)e^{im\varphi}$ allowing the S-L analysis of the radial function $A(r)$ in terms of any family of eigenfunctions defined in the one-dimensional radial coordinate for each given $m$. In a two-dimensional domain, the inner product of two separable functions is also separable. This makes it possible to investigate the resulting one-dimensional inner products separately. For functions not explicitly expressed in a separable form, but defined in a circular domain, they always can be expressed by its circular harmonics [20]. This circular harmonic representation can be done even for nonperiodic functions with the only repercussion that the series converges in the mean [21]. Eigenfunctions are common in mathematical optics; we will use bases of four families of them to engineer optical vortices with tailor-made radial profiles.

### B. Laguerre–Gauss Basis

The LG eigenfunctions are solutions of the paraxial wave equation in cylindrical coordinates $(r, \varphi, z)$ in free space and in quadratic gradient index media [22,23]. These functions are built with the associated Laguerre polynomials and their weighting function $e^{-(x/2)}x^{|m|/2}L_n^{|m|}(x)$. Since their DE is singular at the origin, the zero BC at infinity is needed. Their orthogonality is defined in the interval $[0, \infty)$ with respect to the index $n$ [10,13].

In free space, LG beams are defined by

$$E_{\mathrm{LG}}(r, \varphi, z) = E_0 \frac{w_0}{w(z)} \left( \frac{2r^2}{w^2(z)} \right)^{\frac{|m|}{2}} L_n^{|m|} \left( \frac{2r^2}{w^2(z)} \right) \times \exp\left[ \frac{-r^2}{w^2(z)} - \frac{ikr^2}{2R(z)} + i(2n + |m| + 1)\Phi(z) + im\varphi \right], \tag{3}$$

where the parameters in this equation are the beam waist $w_0$, the beam width $w^2(z) = w_0[1 + (z/R_0)^2]$, the transverse phase front $R(z) = z[1 + (R_0/z)^2]$, and the Gouy phase shift $\Phi(z) = \tan^{-1}(z/R_0)$. In all these expressions $R_0 = kw_0^2/2$ is the Rayleigh distance or diffraction distance for the wavenumber $k = 2\pi/\lambda$. The vortex character is evident through the term showing the azimuthal dependence $e^{im\varphi}$. The parameters $n$ and $m$ are now identified as the radial and azimuthal order of the associated Laguerre polynomials, respectively. These two quantities and the beam waist $w_0$ are control parameters for the radius of the first ring for the LG intensity pattern, as shown in Figs. 1(a) and 1(b).

The fact that the LG beams are free-space modes of the paraxial wave equation allows us to analyze in a straightforward manner the whole propagation of any vortex beam constructed with this basis.

### C. Bessel Basis

The BFs $J_{|m|}(\alpha_m^n x)$ are orthogonal in the unit interval [0,1] for any given order $m$. Since also the Bessel DE has a regular singularity at the origin, only the BC at $x = 1$ is required [10,13]. The value of this BC is zero and the orthogonality is with respect to the eigenvalues $\alpha_m^n (n = 1, 2, \ldots)$, necessary to satisfy the BC at the ends of the aforementioned interval [24,25].

In optics, the BFs appear as the eigenfunctions of the Helmholtz wave equation in circular cylindrical coordinates from which the Bessel vortex beams solutions are represented by [26,27]

$$E_B(x, y, z) = E_0 J_{|m|}(k_r r) e^{ik_z z + im\varphi}. \tag{4}$$

The parameters $k_r$ and $k_z$ are, respectively, the magnitudes of the radial and longitudinal components of the wave vector whose magnitude is $k = 2\pi/\lambda$ and $k_r = \alpha_m^n$. They are related through $k^2 = k_r^2 + k_z^2$. For each element of the basis, it is the azimuthal order $m$ and the radial eigenvalue $k_r$ that determine the radius of the first ring. See Fig. 1(c).

These Bessel beam eigenfunctions can be used to construct a vortex beam with a designed radial intensity profile using a finite number of elements and study the dynamics of its propagation within the distance defined by the maximum frequency used in the expansion [28]. Using a similar approach, the Bessel basis has been successfully proposed as an alternative for studying optical surfaces that occur in visual optics [29].

### D. Zernike Basis

These are the eigenfunctions of an invariant DE in a unitary circular domain investigated by Zernike [30–32] and unlike the previous bases, they satisfy unitary BC at $r = 1$; this is the only one required since the DE also has a regular singularity at the origin. The Zernike circular eigenfunctions are defined by

$$Z_n^m(r, \varphi) = R_n^{|m|}(r) e^{im\varphi}, \tag{5}$$

where $R_n^{|m|}(r)$ are the ZPs with $n$ and $m$, as for the LG, being the radial and azimuthal parameter, respectively. These eigenfunctions are very well known in the study of optical aberrations and can easily be computed to any order [32–34]. An important property of the Zernike basis is that the Hankel transform of a ZP is a BF that is independent of the azimuthal parameter $m$, namely [30,31],

$$\int_0^1 R_n^{|m|}(r) J_{|m|}(\rho r) r \mathrm{d}r = (-1)^{\frac{n-|m|}{2}} \frac{J_{n+1}(\rho)}{\rho}. \tag{6}$$

Notice that the BF on the right-hand side has index $n + 1$, and it is related to the radial index, rather than the azimuthal, which appears in the BF of the integrand on the left-hand side. For Zernike optical fields, the radius of the first ring is determined by the azimuthal order $m$ and the radial eigenvalue $n$. See Fig. 1(d).

Equation (6) has an immediate physical application, once the vortex is constructed, it allows us to find in a forthright way its focused pattern as a superposition of BFs. A further physical outcome is that since the Hankel transform is symmetrical, this relation also hints a method to create arbitrary Zernike optical fields out of modulated Bessel beams.

### E. Fourier Basis

Fourier series are a particular case of a S-L problem that is common to find associated with problems with periodic BCs. We remark here that this is not a requirement but a consequence of the fact that the elements of the basis are periodic functions.

We recall that any function $f(x)$ piecewise square integrable in the symmetric interval $[-l, l]$ can be represented by a Fourier series [11,13]. For the radial coordinate the interval is $[0, a]$ that is obtained by the transformation $r = (a/2l)(x + l)$. Making the substitution $x = ((2/a)r - 1)l$ transforms $f(x) \to F(r)$ and we can write for the elements of the basis

$$\mathcal{F}_n^m(r, \varphi) = (-1)^n \begin{matrix} \cos \\ \sin \end{matrix} \left( \frac{2n\pi}{a} r \right) e^{im\varphi}. \tag{7}$$

In this case, by construction, the radius of the first ring is independent on the azimuthal parameter and depends only on the radial parameter $n$.

## 4. STURM–LIOUVILLE THEORY OF DISCRETIZED EIGENFUNCTIONS

We now express the S-L theory for a sampled function defined in the interval $[a, b]$. For simplicity, let us assume that the $M + 1$ sample points $a \le x_0 < x_1 < \ldots < x_M \le b$ are equally spaced. Using a basis with $N$ elements we can recast Eq. (1) as

$$\mathbf{f} = U\mathbf{c} + \varepsilon_N, \tag{8}$$

where $\mathbf{f}$ is a column vector composed of the ordered sampling of the radial profile to be created; $U$ is the matrix whose elements are $u_{mn} = u_n(x_m)$, with $u_n(x)$ the $n$th eigenfunction of the basis. The vector $\mathbf{c}$ contains the expansion coefficients and the column vector $\varepsilon_N$ represents the rest of the expansion and accounts for the error due to using a finite number of elements in the infinite sum. Since $\{u_n\}$ is an orthonormal basis, the S-L theory guarantees that this is the minimum possible error when approximating $\mathbf{f}$ with $U\mathbf{c}$ and that, even in the worst case of $\mathbf{f}$ not satisfying the same BCs as the basis, it converges in the mean in the least-square sense [11]. By the process of sampling, the problem of obtaining the expansion coefficients has been greatly reduced to a simple matrix inversion.

### A. Applications

To show the usefulness of the present scheme we present two examples that differ considerably from any fundamental vortex beam. The first example is a staircase profile composed by the superposition of two super-Gaussian functions, as shown in the top-left frame in Fig. 2, and its construction using vortex beams with three different topological charges $m = 1, 7, 20$. The rest of the panels in Fig. 2 show the rms error produced by

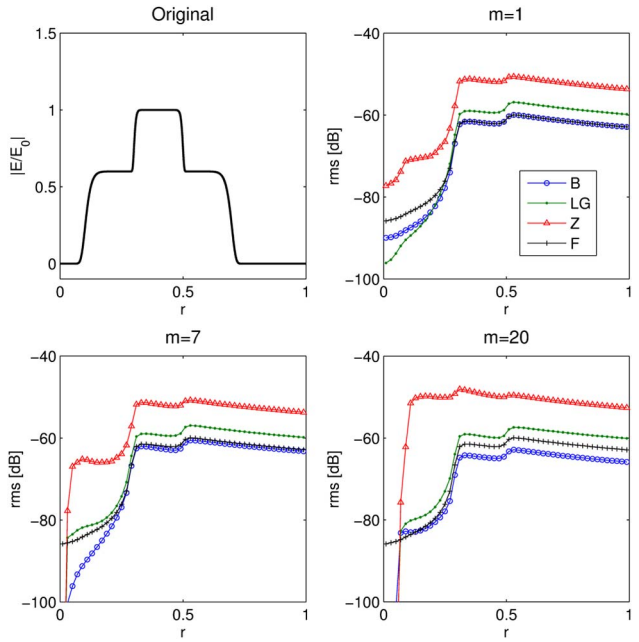


Fig. 2. Composed staircase vortex. The first panel in the top-left corner shows the target profile to be constructed with the proposed scheme, using topological charges $m = 1, 7, 20$. The subsequent panels show the rms approximation error (dB) for Bessel, Zernike, Laguerre–Gauss, and Fourier bases for each topological charge.

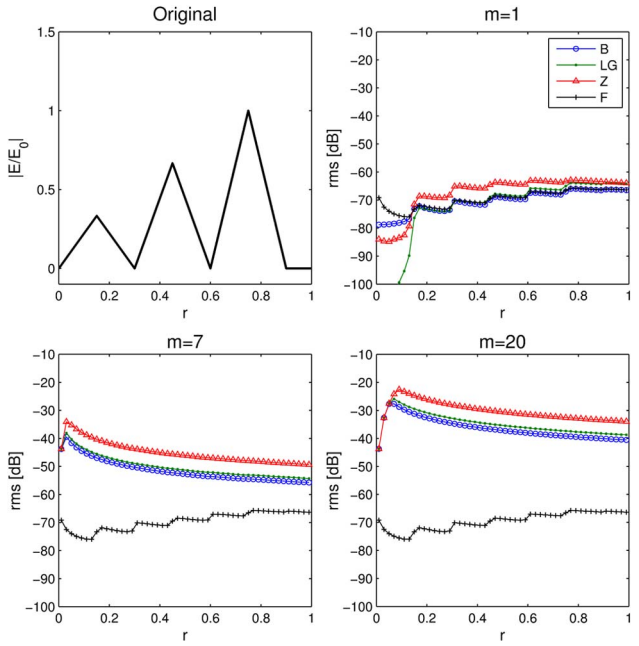


Fig. 3. Intensity of a vortex with sawtooth profile with radially growing amplitude as shown in the first top-left panel. The rest of the panels show the rms error (dB) of the approximations for three topological charges $m = 1, 7, 20$ using Bessel, Zernike, Laguerre–Gauss, and Fourier bases. The Fourier basis performs best, while the B, Z, and LG show a similar behavior.

approximating the profile with 100 eigenfunctions of the Bessel (B), Zernike (Z), Laguerre–Gauss (LG), and Fourier (F) bases. We can see how the Bessel basis converges best to the profile while the Zernike performs worst as expected due to its BCs being different than those of the target profile. Overall, it is seen that the Bessel and Fourier bases behave similarly due to the asymptotic behavior of the former [24,25]. The LG basis has the extra control parameter $w_0$ that allows fine tuning ($w_0 = 0.10$ in the present calculation, notice the use of a normalized range in the examples). There is no rule of thumb for the value of this parameter, it will depend on the profile being approximated [35,36].

As a second example we analyze the engineering of a vortex beam with a more elaborated profile constructed with the same bases and topological charges used in the staircase profile above. In this case we have chosen to design a piecewise continuous sawtooth with a growing profile useful for a uniform, intensity-dependent, transfer of OAM [7]. In the top-left frame of Fig. 3, we show the corresponding sawtooth intensity profile.

This second example is interesting for several aspects. In general, the convergence for all bases is good, as can be seen from the panels in Fig. 3. However, we notice that increasing $m$ results in a deterioration of the convergence near the origin due to the $m$th order polynomial behavior of each basis in that region, making the derivative of the eigenfunctions not satisfy the mixed BCs. Such situation does not occur for the Fourier basis as the expansion is fully independent on $m$, making it perform the best. Nonetheless, the rest of the profile is well approximated with all the bases. Again, it is the Zernike basis that performs the least best for the same reason discussed in the previous example, although the results are not so different from the Bessel and LG bases.

## 5. SUMMARY AND CONCLUSION

In conclusion, based on the S-L theory we have demonstrated that optical vortices can be created with user-designed radial amplitude profile and different topological charges. The engineering of these vortices was performed by the superposition of orthogonal eigenfunctions of optical modes. We have presented examples of vortices with staircase and radially growing sawtooth ringed intensity profiles but our approach can be used for any kind of piecewise amplitude profile. We have investigated four different bases and found that depending on the BCs of the desired profile one basis can be better than the others in approximating the target profile. Three of the bases presented here have the extra feature that can provide physical insight on the propagation, diffraction, or imaging of the created vortex. The scheme proposed here can easily be extended to investigate complex field functions like those created by the inclusion of aberrated optical systems.

## REFERENCES

1. A. M. Yao and M. J. Padgett, "Orbital angular momentum: origins, behavior and applications," Adv. Opt. Photon. **3**, 161–204 (2011).
2. J. Curtis and D. Grier, "Structure of optical vortices," Phys. Rev. Lett. **90**, 133901 (2003).
3. J. P. Treviño, O. López-Cruz, and S. Chávez-Cerda, "Segmented vortex telescope and its tolerance to diffraction effects and primary aberrations," Opt. Eng. **52**, 081605 (2013).
4. K. Dholakia and W. M. Lee, "Optical trapping takes shape: the use of structured light fields," Adv. At. Mol. Opt. Phys. **56**, 261–337 (2008).
5. M. Hartrumpf and R. Munser, "Optical three-dimensional measurements by radially symmetric structured light projection," Appl. Opt. **36**, 2923–2928 (1997).
6. L. Allen, M. W. Beijersbergen, R. J. C. Spreeuw, and J. P. Woerdman, "Orbital angular momentum of light and the

transformation of Laguerre-Gaussian laser modes," Phys. Rev. A **45**, 8185–8189 (1992).
7. K. Volke-Sepulveda, V. Garcés-Chávez, S. Chávez-Cerda, J. Arlt, and K. Dholakia, "Orbital angular momentum of a high-order Bessel light beam," J. Opt. B **4**, S82–S89 (2002).
8. J. A. Hernández Nolasco, "Wave field families of the Helmholtz equation in eleven orthogonal coordinate systems," Ph.D. thesis (INAOE, 2011).
9. H. Feshbach and P. M. Morse, *Methods of Theoretical Physics: Part II* (Cambridge University, 1953).
10. K. T. Tang, *Mathematical Methods for Engineers and Scientists* (Springer, 2007).
11. H. F. Davis, *Fourier Series and Orthogonal Functions* (Dover, 1989).
12. G. E. Andrews, R. Askey, and R. Roy, *Special Functions* (Cambridge University, 2000).
13. M. A. Al-Gwaiz, *Sturm-Liouville Theory and its Applications* (Springer, 2008).
14. H. F. Harmuth, *Transmission of Information by Orthogonal Functions* (Springer, 1970).
15. G. C. G. Berkhout, M. P. J. Lavery, J. Courtial, M. W. Beijersbergen, and M. J. Padgett, "Efficient sorting of orbital angular momentum states of light," Phys. Rev. Lett. **105**, 153601 (2010).
16. M. P. J. Lavery, D. J. Robertson, A. Sponselli, J. Courtial, N. K. Steinhoff, G. A. Tyler, A. E. Wilner, and M. J. Padgett, "Efficient measurement of an optical orbital- angular-momentum spectrum comprising more than 50 states," New J. Phys. **15**, 013024 (2013).
17. E. Karimi, D. Giovannini, E. Bolduc, N. Bent, F. M. Miatto, M. J. Padgett, and R. W. Boyd, "Exploring the quantum nature of the radial degree of freedom of a photon via Hong-Ou-Mandel interference," Phys. Rev. A **89**, 013829 (2014).
18. A. S. Ostrovsky, C. Rickenstorff-Parrao, and V. Arrizón, "Generation of the 'perfect' optical vortex using a liquid-crystal spatial light modulator," Opt. Lett. **38**, 534–536 (2013).
19. M. Chen, M. Mazilu, Y. Arita, E. M. Wright, and K. Dholakia, "Dynamics of microparticles trapped in a perfect vortex beam," Opt. Lett. **38**, 4919–4922 (2013).
20. A. M. Cormack, "Representation of a function by its line integrals, with some radiological applications," J. Appl. Phys. **34**, 2722–2727 (1963).
21. M. V. Berry, "Optical vortices evolving from helicoidal integer and fractional phase steps," J. Opt. A **6**, 259–268 (2004).
22. A. E. Siegman, *Lasers* (University Science Books, 1986).
23. S. Ramo, J. R. Whinnery, and T. Van Duzer, *Fields and Waves in Communication Electronics* (Wiley, 1984).
24. B. G. Korenev, *Bessel Functions and Their Applications* (Taylor and Francis, 2002).
25. G. N. Watson, *A Treatise on the Theory of Bessel Functions* (Cambridge University, 1995).
26. J. Durnin, J. J. Miceli, Jr., and J. H. Eberly, "Diffraction-free Beams," Phys. Rev. Lett. **58**, 1499–1501 (1987).
27. S. Chávez-Cerda, "A new approach to Bessel beams," J. Mod. Opt. **46**, 923–930 (1999).
28. S. Chávez-Cerda, M. A. Meneses-Nava, and J. M. Hickmann, "Interference of traveling nondiffracting beams," Opt. Lett. **23**, 1871–1873 (1998).
29. J. P. Treviño, J. E. Gómez-Correa, D. R. Iskander, and S. Chávez-Cerda, "Zernike vs. Bessel circular functions in visual optics," Ophthalmic Physiolog. Opt. **33**, 394–402 (2013).
30. B. R. A. Nijboer, "The diffraction theory of aberrations," Ph.D. thesis (University of Groningen, 1942).
31. F. Zernike, "Beugungstheorie des schneidenverfahrens und seiner verbesserten form, der phasenkontrastmethode," Physica **1**, 689–704 (1934).
32. V. Lakshminarayanan and A. Fleck, "Zernike polynomials: a guide," J. Mod. Opt. **58**, 545–561 (2011).
33. R. Navarro, R. Rivera, and J. Aporta, "Representation of wavefronts in free-form transmission pupils with Complex Zernike Polynomials," J. Optom. **4**, 41–48 (2011).
34. G. W. Forbes, "Robust and fast computation for the polynomials of optics," Opt. Express **18**, 13851–13862 (2010).
35. J. A. Murphy, "Examples of circularly symmetric diffraction using beam modes," Eur. J. Phys. **14**, 268–271 (1993).
36. J. A. Murphy and A. Egan, "Examples of Fresnel diffraction using Gaussian modes," Eur. J. Phys. **14**, 121–127 (1993).